

Corrosion Study of Clutch Air Spring Gas Circuit under Salt Spray Test

Lin Keng^{1*}, Sun Feng², Zhao JianBin¹, Huang Min¹, Ni RuiYang¹

¹Shanghai Marine Equipment Research Institute, Shanghai 200031, China

²China Ship Development and Design Center, Wuhan 430064, China

DOI: <https://doi.org/10.36347/sjet.2025.v13i02.002>

| Received: 16.12.2024 | Accepted: 21.01.2025 | Published: 03.02.2025

*Corresponding author: Lin Keng

Shanghai Marine Equipment Research Institute, Shanghai 200031, China

Abstract

Original Research Article

This study provides an in-depth analysis of the corrosion resistance of metal products in marine environments, and specifically examines the effectiveness of Type 12S-1 anticorrosive coating in protecting metals in marine environments. The corrosion-resistant behavior of different metal materials under marine conditions is discussed in depth, and a theoretical basis for subsequent simulation experiments is established through electrochemical corrosion theory. This paper focuses on the corrosion performance of clutch air spring airways under different metal materials and conditions of coated or uncoated Type 12S-1 anticorrosive coating, and salt spray tests are used to evaluate and compare the corrosion protection effectiveness of various treatments. The results proved that the 17-4pH material still showed excellent corrosion resistance without coating, and the application of Type 12S-1 anticorrosive coating could enhance the corrosion resistance of the metal to a certain extent. This study not only provides a solid theoretical and empirical foundation for metal anti-corrosion technology in the marine environment, but also provides an important guidance for the optimization of anti-corrosion strategies for ship materials, and provides practical references and directions for the development of related industries.

Keywords: Corrosion resistance of metal products, Salt spray test, Type 12S-1 anticorrosive coating, 17-4 pH Material.

Copyright © 2025 The Author(s): This is an open-access article distributed under the terms of the Creative Commons Attribution **4.0 International License (CC BY-NC 4.0)** which permits unrestricted use, distribution, and reproduction in any medium for non-commercial use provided the original author and source are credited.

1. INTRODUCTION

Atmospheric corrosion, the corrosion of metals in the natural environment of the atmosphere, is a very destructive form of corrosion [1]. The magnitude of its destructiveness is mainly due to the fact that the exposure of metals in the atmospheric environment far exceeds that of other environments [2]. In modern society, large buildings and vehicles, from ships to housing structures, cars, airplanes, etc., are ubiquitous, and they are almost inseparable from our daily lives, and thus are also exposed to atmospheric corrosion at any time [3]. In addition, small metal tools used in everyday life, such as gardening tools, home decorative fences, and exercise equipment, are also under constant threat from atmospheric corrosion [4]. Atmospheric corrosion also has a profound impact on the national economy, especially in coastal cities, where the air contains more corrosive chemicals, leading to more severe metal corrosion, and the resulting maintenance and replacement costs constitute a huge burden on the national economy [5]. Therefore, the study of atmospheric corrosion is not only an important topic in the field of engineering and technology, but also a part of national economic and social development that cannot be ignored.

Atmospheric corrosion is influenced by a number of factors, including ambient temperature, humidity, type and concentration of airborne pollutants, and the nature of the metal and its pretreatment [6]. These factors combine to determine the rate and extent of metal corrosion. In particular, the finish of the metal surface has a particularly significant effect on corrosion. Smooth surfaces make it difficult to form a long-lasting water film, and sometimes even make it difficult for the water film to adhere stably, thus reducing the possibility of electrochemical corrosion [7, 8]. In contrast, rough or uneven surfaces are more susceptible to water film formation and may promote the occurrence of galvanic corrosion even under low relative humidity conditions. This phenomenon highlights the importance of the physical state of the surface in the corrosion process and needs to be emphasized in corrosion protection measures. In recent years, various metal surface corrosion protection materials such as epoxy resin coatings, galvanizing processes and phosphating treatments have proved their effectiveness [9-11], and they are particularly common in corrosion protection environments aiming to improve the adhesion and chemical stability of coatings and thus prevent corrosion by means of different surface treatment techniques.

Anti-corrosive metal coatings have been shown to be particularly effective in marine metal corrosion protection by forming a protective layer on the metal surface to isolate corrosive media (e.g., water, oxygen, and salt) and prevent them from coming into direct contact with the metal substrate [12]. These coatings not only provide physical isolation but also inhibit or slow down the corrosion process through chemical stability [13, 14]. Although existing anticorrosion coatings have demonstrated good protection in practical applications, they still face some challenges, such as long-term stability of coatings, environmental adaptability, and adhesion to metal substrates [15]. In addition, as environmental regulations tend to be more stringent, there are higher requirements for volatile organic compound (VOC) emissions from coatings, which has prompted researchers to explore more environmentally friendly formulations for anticorrosion coatings [16, 17].

Understanding the response of different metallic materials to atmospheric corrosion is essential when evaluating the effectiveness of corrosion protection measures [18, 19]. Various metallic materials exhibit different corrosion resistance; therefore, the relevance and efficiency of anti-corrosion techniques can be significantly improved by selecting different metals for comparative corrosion tests. For example, copper and aluminum have high corrosion resistance due to their ability to form a protective oxide layer [20], on the contrary, iron and steel are prone to rust formation in humid environments, which accelerates the corrosion process [21]. In addition, alloying studies have shown that the resistance to atmospheric corrosion can be enhanced by adjusting the ratio of elements in the alloy composition [22, 23]. Therefore, targeted corrosion mechanism studies and long-term environmental exposure tests on metals and alloys not only help to understand the details of the corrosion process, but also serve as an important basis for the development of new and efficient corrosion resistant materials and technologies. Through these studies, we are able to design metal materials and corrosion prevention programs for industrial applications that are more adaptable to specific environmental conditions, effectively extending the service life of metal structures and reducing maintenance costs.

This paper focuses on the corrosion resistance of clutch air spring air paths in marine environments. The harsh conditions of the marine environment make the existing corrosion resistance measures seem insufficient, therefore, this study aims to explore and improve these technologies. The paper is arranged as follows: Section II exhaustively analyzes the electrochemical theory of metal corrosion, which provides a solid theoretical basis for the subsequent simulation experiments, Section III explores the electrochemical corrosion and corrosion thickness changes under different material combinations through corrosion simulation salt spray experiments, Section IV carries out a salt spray test for different metal

materials and whether or not to apply Type 12S-1 anticorrosive coating in order to assess the various anti-corrosion treatments as well as the actual anti-corrosion effects of different metal materials, the last section summarizes the research results and presents several preliminary conclusions. Through these systematic studies, this paper aims to provide scientific basis and practical guidance for the development of corrosion resistance technology in marine environment.

2. Electrochemical behavior of metal corrosion

In the study of metal corrosion, temperature variations are closely linked to changes in the concentration of substances, which together influence the electrochemical behavior of corrosive media [24]. The transport of heat and substances generated by electrochemical reactions during corrosion can be described by a number of equations that reveal how these two transport phenomena act jointly in the corrosion process [25].

First, let us consider the mass-transport flow J , which forms at the interface between a metal surface and a corrosive medium and is driven by a concentration gradient and a temperature gradient [26]

$$J = -sD \left[\frac{\partial c}{\partial x} + \kappa_s \left(\frac{\partial \ln(\theta)}{\partial x} \right) + \kappa_s \frac{\partial \sigma}{\partial x} \right], \dots \dots \dots (1)$$

where s is the reaction rate coefficient, which represents the rate at which a substance is produced or consumed, D is the diffusion coefficient, which describes the ability of a substance to diffuse due to a concentration gradient, c is the concentration of the substance in the medium, whereas κ_s is the thermodiffusion coefficient, which correlates the temperature gradient and the rate of substance migration, θ represents the local temperature, and σ is the specific entropy. This equation not only captures the effect of the concentration gradient on the mass transport flow, but also incorporates the possible effect of the temperature gradient (Soret effect) as well as the change in specific entropy on the corrosion rate.

The thermal diffusion coefficient κ_s describes the effect of a temperature gradient on mass transport flow, which is related to the thermophysical properties of the substance

$$\kappa_s = \frac{C}{s} \times \frac{V_H}{R(\theta - \theta')}, \dots \dots \dots (2)$$

here C is the specific heat capacity, V_H is the partial molar volume, R is the ideal gas constant and θ' is the reference temperature. During the corrosion process, local temperature changes may lead to changes in the concentration distribution of the corrosive medium, affecting the corrosion rate.

When considering the effect of temperature gradients on electrochemical corrosion, the above equations can be combined with the concept of electrochemical potential. The rate of an electrochemical

reaction may vary depending on the temperature because the temperature directly affects the activation energy of the reaction

$$\frac{d\mu}{dT} = -\sigma, \dots\dots\dots (3)$$

here μ represents the electrochemical potential, which is related to the migration of metal ions in the electrolyte solution as well as their adsorption and desorption at the electrode surface. Therefore, the electrochemical corrosion rate is not only affected by the mass transport flow, but also by the change in electrochemical potential caused by the temperature gradient.

In summary, the electrochemical corrosion rate can be described by a comprehensive model that takes into account the effects of concentration gradients, temperature gradients, and specific entropy changes on the corrosion rate of metals:

$$J = -sD \left[\frac{\partial c}{\partial x} + \kappa_s \left(\frac{\partial \ln(\theta)}{\partial x} \right) + \kappa_s \frac{\partial}{\partial x} \left(-\frac{d\mu}{dT} \right) \right] \dots\dots (4)$$

Let's assume that the change in the assumed temperature gradient θ relative to the reference state θ' is small, then there is:

$$\ln(\theta) \approx \ln(\theta') + \frac{\theta - \theta'}{\theta'} \dots\dots\dots (5)$$

Assuming that the diffusion process is not very dependent on the entropy change, or that the gradient is smaller than the entropy over the range considered for temperature, then $\frac{\partial \sigma}{\partial x}$ can be ignored. Based on these assumptions, we can simplify Eq. (1) to

$$J = -sD \left[\frac{\partial c}{\partial x} + \kappa_s \frac{\theta - \theta'}{\theta'} \right] \dots\dots\dots (6)$$

3. Clutch air spring gas circuit corrosion simulation study

In this section, we will carry out a simulation study of the corrosion of the clutch air spring gas circuit. Through simulation experiments, we aim to deeply investigate the corrosion characteristics of the clutch air spring air circuit, which lays a solid theoretical foundation for subsequent experimental studies. This process not only helps to predict the corrosion trend, but also provides an important reference for taking effective anti-corrosion measures.

We study the corrosion behavior of clutch air spring airways in marine environments. To simulate

marine environments, we designed a salt spray test in which the corrosion process is significantly driven by humid atmospheric conditions, and salt particles become the dominant factor of corrosion [27]. The test components mainly consisted of two parts, the substrate and the cover, and the corrosion mechanism was mainly presented as electrochemical corrosion due to the difference in their material compositions. In this mechanism, the anodic region tends to undergo oxidation reaction and exhibits a low equilibrium potential, while the cathodic region undergoes reduction reaction and has a high equilibrium potential [28]. Based on the specific environment of the experiment, we designed three experimental groups:

Group I: The base body is made of 35CrMo material, the sealing plate is made of Q235 material, and the surface is not treated with anti-corrosion.

Group II: The base body is made of 35CrMo material, the sealing plate is made of 17-4pH material, and the surface is not treated with anti-corrosion.

Group III: The substrate is made of 17-4pH material, the closure plate is made of 17-4pH material, and the surface is not preserved.

In the present study, we performed a detailed simulation analysis of three different working conditions using the electrochemical corrosion module. In the simulated environment, the substrate material, which acts as the anode, undergoes iron oxidation, and this process produces rust, whose main components include iron dioxide (Fe_2O_3) and iron hydroxide ($Fe(OH)_3$) [29]. In contrast, the cover material, which is the cathode, undergoes a reduction reaction, which is mainly characterized by the precipitation of iron. The purpose of this simulation study is to understand in detail the behavior of the material during the electrochemical corrosion process, and then guide the experimental design and optimize the corrosion protection strategy.

The object of study in this section is the clutch air spring air circuit, which is mainly composed of two parts: the base body and the cover plate. Based on the specific dimensional data of the base body and the cover plate cross-section of the clutch air spring air circuit, we design the simulation model as a twodimensional planar strain model, and the specific model schematic is shown in Fig. 1, with the red area representing the cover plate as the cathode, and the other areas are the base body acting as the anode.

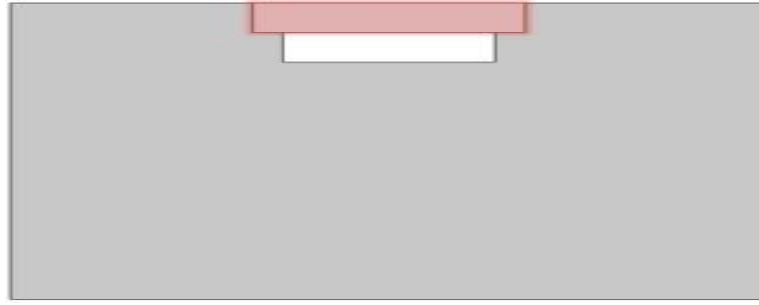


Figure 1: Global phase portraits of Case 3

The simulation covered a period of three days and was aimed at evaluating the corrosion behavior under three different material combinations. The simulation results are shown in Fig. 2 for electrolyte potential, Fig. 3 for electrolyte current density, Fig. 4 and for the relationship between electrode potentials and neighboring reference potentials. Considering the steady

state nature of the corrosion process, we provide simulation results after 24 hours of corrosion. The comparative analysis of these results allows us to reveal the differences in the behavior of different material combinations in electrochemical corrosion environments, which are important guides for the development of future corrosion protection measures.

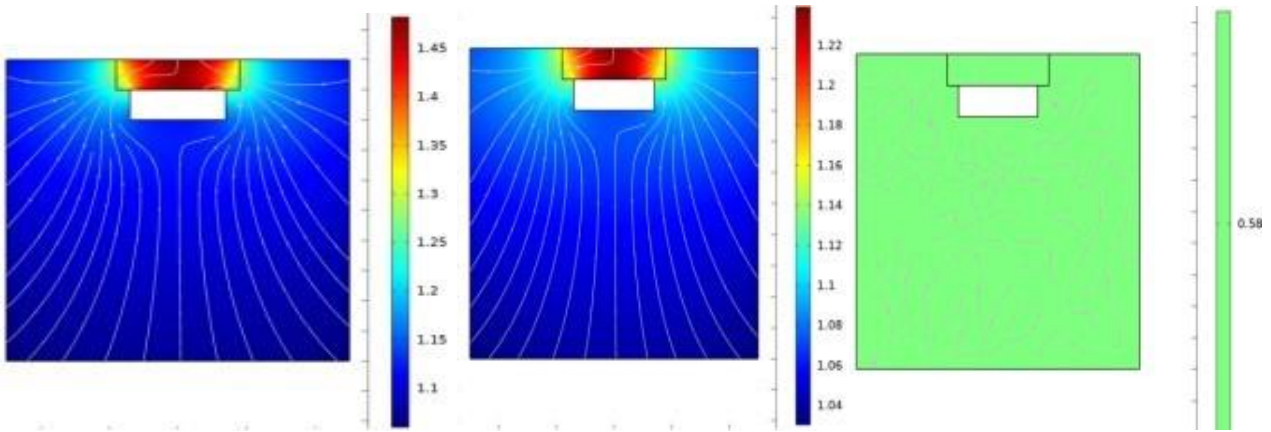


Figure 2: Electrolyte potentials (in V) corresponding to the three experimental groups

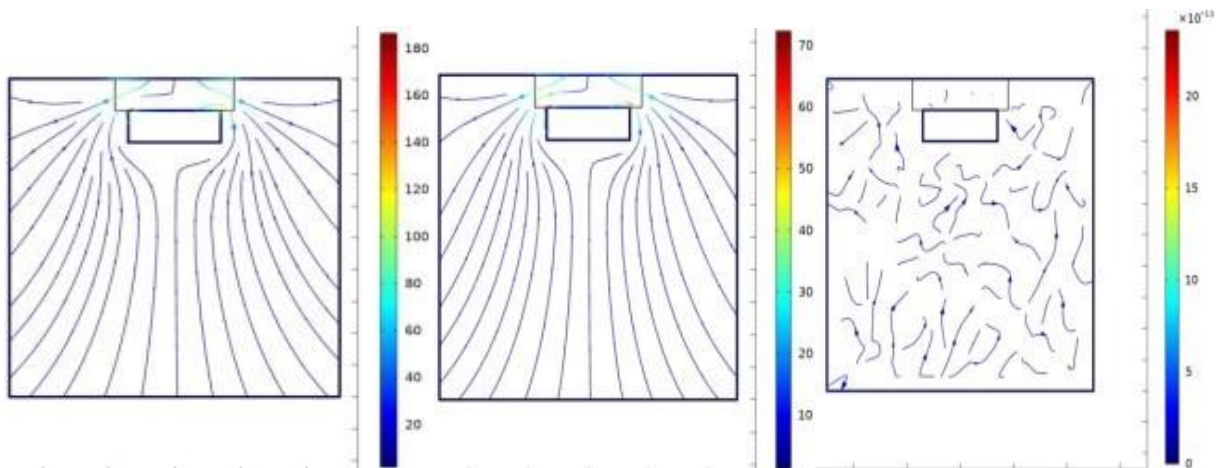


Figure 3: Corresponding electrolyte potentials (in V) for the three experimental groups

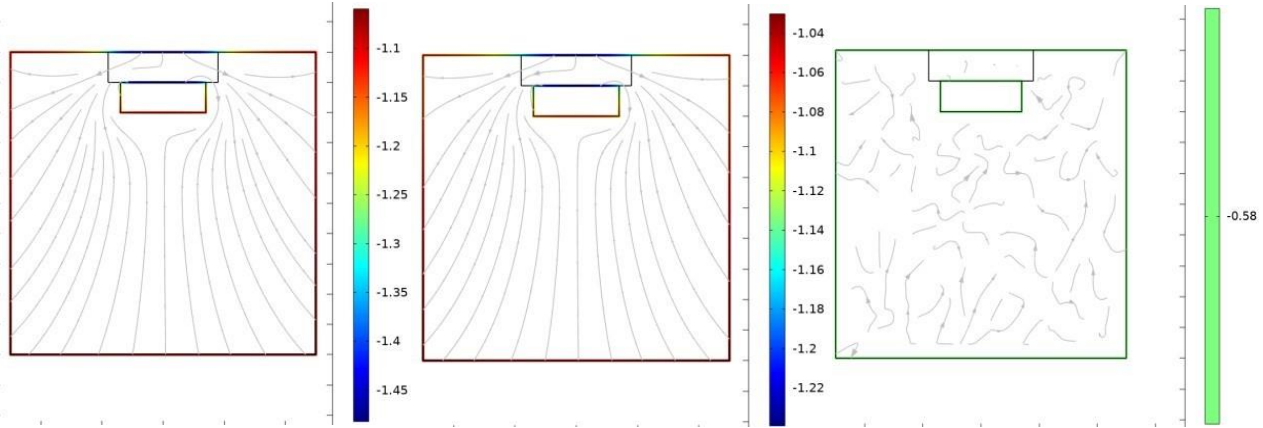


Figure 4: Electrolyte current density (in A/m^2) for three experimental groups

By analyzing the above simulation results in depth, we can come up with the following findings: in both the first and the second group, the system develops a stable potential difference and establishes a current distribution with a clear direction. This distribution indicates that the current flows from the cover (cathode) to the substrate (anode), thus constituting a primary cell effect that results in the substrate as an anode being more susceptible to corrosion. The rate of corrosion of the substrate during this process can be assessed by measuring the current density in the electrolyte. In the third group, on the other hand, due to the uniformity of the anode and cathode materials, the formed current density is extremely small and almost negligible, which indicates that the corrosion behavior is effectively suppressed in the case of homogeneous materials [30].

The magnitude and direction of this current density not only reflect the level of corrosion activity, but also reveal the pathway of electron transfer during the corrosion process. When there is a difference between the substrate and cover materials, due to the difference in electrochemical properties, it is easy to form a difference

in electrochemical potential, thus accelerating the corrosion process of the anode [31]. On the contrary, when both materials are the same and are untreated against corrosion, the potential difference decreases and electron transfer is hindered, thus reducing the tendency of corrosion [32]. These findings are important in guiding how to select materials and design structures to enhance corrosion resistance, and provide theoretical predictions and references for subsequent more detailed experimental studies.

Continuing to deepen our study, we will observe the changes in material thickness after 24, 48, and 72 hours of corrosion. Changes in corrosion thickness not only reflect the corrosion rate, but may also reveal differences in material resistance to corrosion, the dynamic evolution of the corrosion process, and possible corrosion mechanisms [33]. By determining the corrosion thickness at different time points, we are able to construct a time series model of the decay of material properties in corrosive environments, thus providing predictions of the long-term stability and durability of materials.

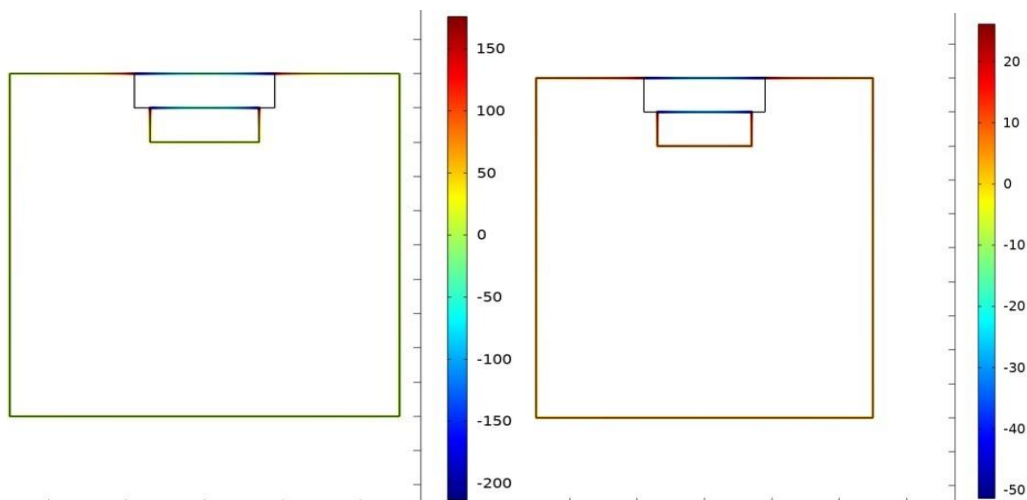


Figure 5: Corrosion thickness variation between the first and second group corresponding to 24 hours

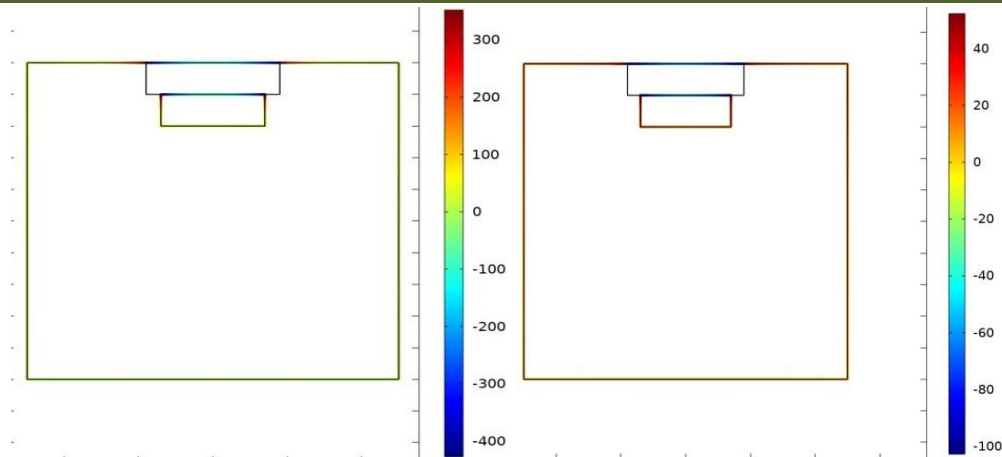


Figure 6: Corrosion thickness variation between the first and second group corresponding to 48 hours

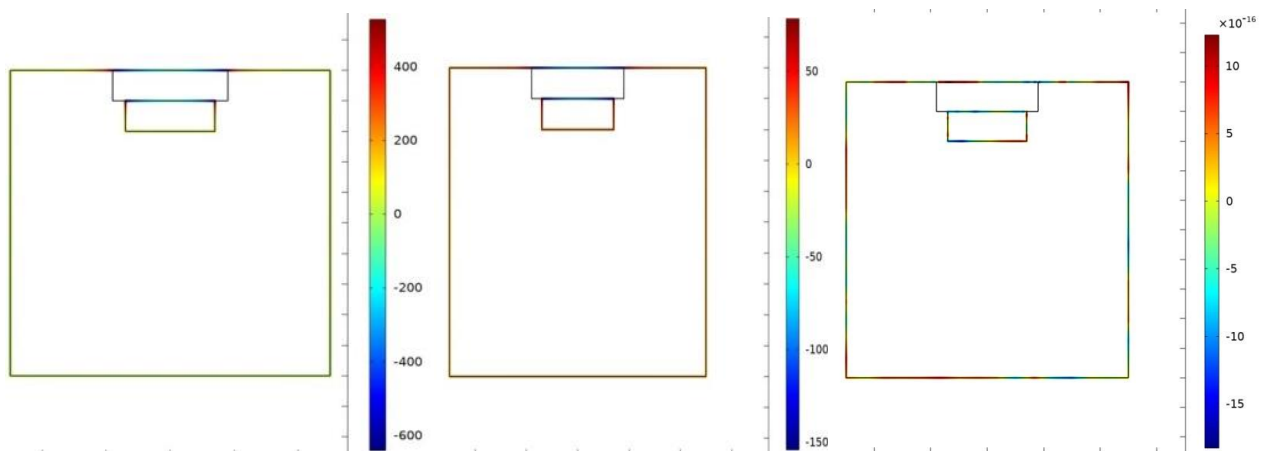


Figure 7: Corrosion thickness variation corresponding to 72 hours for three experimental groups

In the charts provided, the changes in corrosion thickness after 24, 48, and 72 hours for three different groups are shown in detail. In these graphs, the decrease in thickness at the anode reflects the oxidation of the ferrous material to rust, while the increase in thickness at the cathode shows the conversion of ions in the electrolyte to metallic iron through a reduction reaction. This change in thickness was evident in the first and second groups, especially by the third day, when the amount of change reached the micrometer level. In contrast, the change in thickness in the third group was extremely small and almost negligible, mainly due to the failure to form an effective protocell structure in this experimental group, and hence the extremely low amount of electrochemical reaction that occurred. This indicates that the 17-4pH material has better corrosion resistance than the 35CrMo and Q235 materials, and that the 17-4pH material has a corrosion resistance of at least more than three days in seawater bad conditions.

4. Experimental study of corrosion in the air circuit of clutch air springs

The chemical and physical properties of different metallic materials themselves can have an impact on the corrosion protection [34]. Indeed, the wide variety of metallic materials used in industrial production makes it particularly critical to compare the corrosion

protection properties of different products and materials, whether coated with corrosion protection materials or not. Therefore, an indepth study of these differences is essential to understand and optimize corrosion protection measures.

In this paper, we use 12S-1 anticorrosive coating, whose main components include film-forming substances: polytetrafluoroethylene (PTFE), waterborne polyurethane resin (PUR), film-forming auxiliaries: dispersing agent, leveling agent, defoamer and dispersing medium: deionized water, co-solvent, etc. PTFE is a linear crystalline polymer, whose hydrogen atoms have been replaced by fluorine atoms to form a nonpolar, inert helical shell, which endows it with excellent chemical corrosion protection. PTFE is chemically very stable and suitable for long-term resistance to chemical attack [35, 36]. PUR is widely used in coatings as a customizable polymer resin with the advantages of hardness, flexibility, abrasion resistance and strong adhesion. Waterborne polyurethanes replace conventional organic solvents with water, which reduces the release of harmful volatile organic compounds and makes the coatings more environmentally friendly and safe [37]. In addition, the low-temperature curing characteristics of these coatings reduce energy

consumption and meet the needs of modern industrial production [38].

A waterborne polyurethane resin (PUR) with a solid mass fraction of 0.5 was added to N, N-dimethylethanolamine with a mass of 7% to 8% and the pH was adjusted to 7.5 to 8.5. Next, an aqueous wetting and dispersing additive, a portion of the co-solvent and a portion of the de-ionized water were added to make a mixture with a fineness of no more than 10m by a sanding process. Subsequently, an aqueous polytetrafluoroethylene (PTFE) emulsion was added, remaining co-solvent, remaining deionized water and other additives, adjusting the stirring speed to 800 rpm and continuing the dispersion for 15 minutes to produce 12S-1 anticorrosive coating.

In order to further study metal corrosion in depth and verify the conclusions drawn from the previous corrosion simulation, the object of study in this section is the clutch air spring air circuit, and the metal materials involved include 35CrMo, Q235 and 17-4pH. The anti-corrosion material used in the experiment is the Type 12S-1 anticorrosive coating, and in order to simulate the use of the product in the marine atmosphere, we use a salt spray test. The experiment uses SK-110C salt spray constant temperature and humidity composite test chamber, the experimental temperature is set to 45 °C, the use of salt spray is 5% concentration of brine, and the sedimentation rate is set to 2 ml per hour, the use of continuous spraying, in order to match with the actual,

we set the test cycle of 18 days. The experimental process is as follows: we put the test piece into the test chamber, observe and take pictures every day, and clean the test piece every three days to observe the corrosion situation more clearly, observe and take pictures. Finally the end of the test is clear, observed and photographed. The whole study is divided into four experimental groups:

Group I: The base body is made of 35CrMo material, the sealing plate is made of Q235 material, and the surface is not treated with anti-corrosion.

Group II: The base body is made of 35CrMo material, the sealing plate is made of Q235 material, and the surface is coated with Type 12S-1 anticorrosive coating.

Group III: The substrate is made of 35CrMo material, the sealing plate is made of 17-4pH material, and the surface is not treated with anti-corrosion.

Group IV: The substrate and closure plate are made of 17-4pH material and the surface is not preserved.

Fig. 8 shows the state of five sets of test pieces before the experiment. Through these configurations, the corrosion behavior under different material combinations is compared and the corrosion resistance of Type 12S-1 anticorrosive coating is evaluated on the surfaces of different materials. These experimental setups help to understand the corrosion resistance of various materials in practical applications and provide a scientific basis for future material selection and surface treatment.



Figure 8: Clutch air spring gas line pins before salt spray test



Figure 9: Clutch air spring air circuit after one day of salt spray test



Figure 10: Clutch air spring gas line plug after four days of salt spray test



Figure 11: Clutch air spring gas line spigot status after thirteen days of fog test



Figure 12: Clutch air spring gas line plug after eighteen days of salt spray test



Figure 13: Corrosion of three sets of test pieces (after cleaning)

Fig. 9 shows the state of the test pieces on the first day of the experiment, the first group of test pieces appeared localized corrosion phenomenon, while the second group of test pieces also occurred localized corrosion, but to a lesser extent than the first group, this result proves the effectiveness of the Type 12S-1 anticorrosive coating on the 35CrMo and Q235 materials. In the third group, localized corrosion occurred on the substrate, while no corrosion was

observed on the sealing plate, indicating that the 17-4pH material has better corrosion protection than Q235, and its effect even exceeds that of Q235 coated with anticorrosion coating, which suggests that the 17-4pH material is well suited to seawater environments due to its excellent corrosion protection properties. The fourth group showed no corrosion at all, further indicating that 17-4pH is superior to 35CrMo in terms of corrosion resistance, and even outperforms 35CrMo coated with

anticorrosive coatings, making it a more ideal material choice for seawater environments.

Fig. 10 shows the status of the test pieces on the fourth day of the experiment. The first group of test pieces showed uniform corrosion, indicating that the test pieces were uniformly damaged at the same rate, with the 35CrMo substrate and the Q235 sealer showing similar corrosion conditions and no prominent localized damage on the material surface. The second set of test specimens showed localized corrosion, but less severe than the first set, further confirming that the Type 12S-1 anticorrosive coating continue to exhibit corrosion protection over time. The third set of test specimens showed uniform corrosion, but no corrosion of the sealing plate, demonstrating that the 17-4pH material maintains 100% corrosion protection after four days in a 5% salt spray environment. The fourth group of test pieces has not experienced any corrosion so far, further verifying the excellent anti-corrosion performance of 17-4pH material.

Fig. 11 demonstrates the state of the test pieces on the thirteenth day of the experiment, with uniform corrosion occurring in both the first and second groups of test pieces. This shows that even with the Type 12S-1

anticorrosive coating, the 35CrMo and Q235 materials still corrode severely after prolonged exposure to a 5% concentration of salt spray. Uniform corrosion occurred on the substrate in the third group, while no corrosion occurred on the sealer plate, again demonstrating the excellent corrosion protection of the 17-4pH material. The fourth group has not experienced corrosion to date, which further emphasizes the excellent corrosion protection of the 17-4pH material when continuously exposed to a 5% salt spray concentration. These observations highlight the differences in performance of different materials and corrosion treatments under extreme conditions.

Fig. 12 shows the state of the test pieces on the eighteenth day of the experiment, which is also the last day of the experiment, and the corrosion conditions of the test pieces in each group are as follows: uniform corrosion occurred in both the first and second groups. The substrate in the third group also corroded uniformly, while its sealing plate did not show any signs of corrosion. In the fourth group, no corrosion has occurred so far. Finally, the test pieces were cleaned, and Fig. 13 shows the final corrosion of the first, second, and third groups of test pieces after cleaning.

Table 1: Substrate corrosion

Corrosion	Group I	Group II	Group III	Group IV
Localized corrosion	1 day	1 day	1 day	No corrosion
uniform corrosion	4 day	13 day	4 day	No corrosion

We list Table 1 summarizes the occurrence of corrosion in each group of test pieces, from Table 1 and eighteen days of corrosion can be seen in the third group of substrate than the first group of corrosion is serious, the reason is that the third group of test pieces of part of the material is used 17-4pH material, the material and the substrate of 35CrMo material galvanic corrosion, exacerbating the corrosion rate of the substrate [39, 40], the second group (coated with anticorrosive coating), the number of days in which uniform corrosion of the substrate occurred was 13 days, which increased the corrosion protection life by more than three times compared with the 4 days in the first group (without anticorrosion treatment), there was no corrosion in the third group of sealing plates (made of 17-4pH) and the fourth group as a whole (made of 17-4pH) during the test.

We summarize the corrosion life of these four groups of experiments: Group I (no anti-corrosion treatment): corrosion life of 1 day, Group II (coated with anticorrosion coatings): corrosion life increased dramatically to 13-15 days, Group III (sealing plate made of 17-4pH): corrosion life of the substrate is 4 days; the sealing plate life is greater than 18 days, but the substrate corrosion is accelerated, Group IV (airway made of 17-4pH): life of the airway is greater than 18 days, but matrix corrosion accelerated, Group V (overall 17-4pH manufacture): overall life greater than 18 days.

The results of this experiment clearly demonstrate the superior corrosion resistance of the 17-4pH material, which maintains excellent stability even after long-term exposure to corrosive environments. At the same time, the experiments also showed that Type 12S-1 anticorrosive coating are effective in resisting corrosion in the short term. These findings provide an important basis for selecting materials and anti-corrosion treatments that are suitable for specific environmental conditions.

5. CONCLUSION

This paper looks at the phenomenon of corrosion of metallic materials in the atmosphere and the effectiveness of metallic anti-corrosion coatings. By designing a reasonable salt spray test to simulate the influence of the marine environment, we have carried out the simulation of clutch air spring air circuit corrosion with different metal materials. By comparing the corrosion thickness of test pieces under different materials, we verify the corrosion prevention effectiveness of 17-4pH materials in seawater. Further, a more detailed salt spray test was designed using different metal materials and Type 12S-1 anticorrosion coating. The clutch air spring airway was divided into five experimental groups and the differences in the corrosion effects of whether or not the Type 12S-1 anticorrosion

coating was applied were examined. With 18 days of continuous observation and documentation, the results showed that the 17-4pH material demonstrated excellent corrosion resistance in a simulated marine environment. At the same time, these tests confirmed the ability of Type 12S-1 anticorrosion coating to effectively resist corrosion in the short term. These findings not only provide a scientific basis for material selection and corrosion protection, but also provide an important reference for future related research.

REFERENCES

- George D. de la Fuente, I. D'iaz, J. Simancas, B. Chico, M. Morcillo. Longterm atmospheric corrosion of mild steel. *Corrosion Science*. 2011, 53(2): 604-617.
- Yingwei Song, Jiaming Dai, Shuo Sun: A comparative study on the corrosion behavior of AZ80 and EW75 Mg alloys in industrial atmospheric environment. *Materials Today Communications*. 2024, 108263(38): 2352- 4928.
- Haiying Wu, Yaozhi Luo, Guangneng Zhou: Corrosion behaviors and mechanical properties of Q235 steel pipes collapsing due to corrosion after 25year service in urban industrial atmospheric environment. *Construction and Building Materials*. 2023, 359: 132342.
- Guanghua Wan, Dongqing Zhu, Chen Wang, Xun Zhang: Atmospheric corrosion of T2 copper and H62 brass exposed in an urban environment. *Materials Chemistry and Physics*. 2023, 299: 127487.
- Daquan Zhang, Zixuan Yan, Lixin Gao, Zhiling Xin, Yongxin Zhu, Wei Wu: Corrosion behavior of AA5052 aluminum alloy in the presence of heavy metal ions in 3.5 % NaCl solution under negative pressure. *Desalination*. 2024, 570: 117082.
- Jua Kim, Haobo Pan: Effects of magnesium alloy corrosion on biological response Perspectives of metal-cell interaction. *economics Letters*. 2023, 133: 101039.
- Jiheon Jun, Vineet V. Joshi, Alasdair Crawford, Vilayanur Viswanathan, Donovan N. Leonard, Jian Chen, Piyush Updadyay, Yong Chae Lim. Zhili Feng: Galvanic corrosion of AZ31B joined to dual-phase steel with and without Zn layer by ultrasonic and friction stir welding. *Journal of Magnesium and Alloys*. 2023, 11(2): 462-479.
- Tiansui Zhang, Zhengyun Wang, Yubing Qiu, Tayyaba Iftikhar, Hong-fang Liu: "Electronsiphoning" of sulfate reducing bacteria biofilm induced sharp depletion of Al, Zn, In, Mg, Si sacrificial anode in the galvanic corrosion coupled with carbon steel. *Corrosion Science*. 2023, 216: 111103.
- Chandrabhan Verma, Lukman O.asunkanmi, Ekemini D. Akpan, M.A. Quraishi, O. Dagdag, M. El Gouri, El-Sayed M. Sherif, Eno E.Ebenso: Epoxy resins as anticorrosive polymeric materials: A review. *Reactive and Functional Polymers*. 2020, 156: 104741.
- Bo Yang, Wenlong Zhen, Jiantai Ma, Gongxuan Lu: Corrosion inhibition and stability enhancement of cobalt phosphide in aqueous solution by coating TiO₂ layer. *International Journal of Hydrogen Energy*. 2023, 48(94): 3678436794.
- Yongsheng Liu, Haiyang Gao, Hao Wang, Xin Tao, Wanzhi Zhou: Study on the corrosion behavior of hot-dip galvanized steel in simulated industrial atmospheric environments. *International Journal of Electrochemical Science*. 2024, 19(1): 100445.
- O.S.I. Fayomi, A.P.I. Popoola, V.S. Aigbodion: Investigation on microstructural, anti-corrosion and mechanical properties of doped Zn-Al-SnO₂ metal matrix composite coating on mild steel. *Journal of Alloys and Compounds*. 2015, 623: 328-334.
- Jaehoon Joo, Minjoo Kang, Hyoung-Seok Moon, Sanghyuk Wooh, Junghoon Lee: Design and experimental studies of self-healable anticorrosion coating: Passivation of metal surfaces by silicone oil impregnated porous oxides. *Surface and Coatings Technology*. 2020, 404: 126595.
- V.S. Benitha, K. Jeyasubramanian, G.S. Hikku: Investigation of anticorrosion ability of nano mixed metal oxide pigment dispersed alkyd coating and its optimization for A36 steel. *Journal of Alloys and Compounds*. 2017, 721: 563-576.
- A.M. Fadl, M.I. Abdou, Doaa Laila b, S.A. Sadeek: Fabrication and characterization of novel p-Phenylamine-N (4-chloro salicylaldenimine) ligand and its metal complexes and evaluation their anti-corrosion and chemical resistance properties in epoxy/SiO₂ nanocomposite for steel surface coating. *Chemical Engineering Journal*. 2020, 384: 123390.
- Di Yin, Zongxue Yu, Legang Chen, Kunyao Cao: Enhancement of the AntiCorrosion Performance of Composite Epoxy Coatings in Presence of BTAloaded Copper-Based Metal-Organic Frameworksi. *International Journal of Electrochemical Science*. 2019, 14(5): 4240-4253.
- Amir Hossein Mostafatabar, Ghasem Bahlakeh, Bahram Ramezan-zadeh: Designing a novel anti-corrosion metal-organic platform based on dual-action epoxy coating. *Progress in Organic Coatings*. 2022, 170: 107007.
- Yi Wang, Guanglong Li, Hao Qi, Wei Zhang, Ruirun Chen, Ruiming Su, Bo Yu, Yingdong Qu: Effect of non-metallic carbon content on the microstructure and corrosion behavior of Al-Co-Cr-Fe-Ni high-entropy alloys. *Intermetallics*. 2024, 166: 108181.
- Gopinath Shit, S. Ningshen: Effect of metallic redox ions on the corrosion behavior of GTAW weldment of type 304L stainless steel in simulated nonradioactive PUREX and HLLW medium. *Progress in Nuclear Energy*. 2024, 168: 105039.
- Eakambaram Arumugam, Sivakumar Solaiachari: Experimental analysis and machining

- characterization of aluminium 356 matrix composites reinforced with fly ash and alumina oxide Al₂O₃. *Journal of Economic Perspectives*. 2023, 7: 2214-7853.
21. Kuangyu Dai, Shengli Li, Pengyue Hu, Nan Jiang, Dongwei Wang: Effect of outer rust layer on cathodic protection and corrosion behavior of highstrength wire hangers with sheath crack in marine rainfall environment. *Case Studies in Construction Materials*. 2023, 18: e02043.
 22. Yonghua Chen, Liang Wu, Xiaoxiao He, Wenhui Yao, Jiahao Wu, Yuantai He, Yan Zhou, Yuan Yuan, Jingfeng Wang, Zhihui Xie, Andrej Atrens, Fusheng Pan: Corrosion resistance study of ZIF-67/Co-Fe LDHs composite coating on the surface of AZ31 magnesium alloy micro arc oxidation film. *Journal of Alloys and Compounds*. 2024, 989: 174278.
 23. Ankit Kumar, Gurminder Singh : Surface modification of Ti6Al4V alloy via advanced coatings: Mechanical, tribological, corrosion, wetting, and biocompatibility studies. *Journal of Alloys and Compounds*. 2024, 989: 174418.
 24. Xin Zhang, WanMei, Zehua Zhou, Shaoqun Jiang, Gang Wang, Xiangru Shi, Zehua Wang : Galvanic corrosion behavior of AZ91D alloy / 45 steel couple under magnetic field. *Journal of Magnesium and Alloys*. 2023, 3: 2213-9567.
 25. Mengyuan Huang, Norbert Weber and Gerd Mutschke: A Simulation Framework for Electrochemical Processes with Electrolyte Flow. *Journal of The Electrochemical Society*. 2023, 170: 073502.
 26. Stansbury, E. E., Buchanan, R. A. *Fundamentals of Electrochemical Corrosion*. ASM International. 2020.
 27. Naeemeh Esfandiari, Mahmood Aliofkhaezrai, Alejandro Nicol'as ColliJaeyoung Lee: Comparative corrosion analysis of acrylic precoated aluminum foil under natural exposure and neutral salt-spray (NSS) testing. *International Journal of Electrochemical Science*. 2023, 18(12): 100373.
 28. Miaoran Liu, Huang Peng, Youji Tao, Jun Wang, Ganxin Jie: Cathodic corrosion to fabricate Au electrodes with unique properties for single-crystal electrochemistry, electrocatalysis, and SER spectroscopy. *Encyclopedia of Solid-Liquid Interfaces*. 2024: 473-485.
 29. Shedrack Musa Gad, Xiaorong Zhou, Stuart B. Lyon: Inhibition mechanism of anticorrosion pigments leached from organic coatings: Comparison between salt spray and immersion testing. *Progress in Organic Coatings*. 2023, 174: 107266.
 30. Meng Cao, Zhang-Zhi Shi, Jin-Ling Sun, Zhen Li, Lu-Ning Wang: Threestage degradation behavior and dealloying assisted galvanic corrosion mechanism of 300 MPa grade Zn-2Cu-xLi (x = 0.2-0.8) alloys in simulated body fluid. *Corrosion Science*. 2024, 228: 111818.
 31. Zhi-Hui Xie, Dan Xu, Ya Shu, Qiwen Yong, Liang Wu, Gang Yu: Environmentally friendly and facile Mg(OH)₂ film for electroless nickel plating on magnesium alloy for enhanced galvanic corrosion inhibition. *Surface and Coatings Technology*. 2024, 479: 130371.
 32. Huixin Zhu, Zhiyong Huang, Guofeng Jin, Mingna Gao: Effect of temperature on galvanic corrosion of Al 6061-SS 304 in nitric acid. *Energy Reports*. 2022, 8(14): 112-123.
 33. Muhammad Ahsan Iqbal, Endzhe Matykina, Raul Arrabal, Marta Mohedano: Role of anodic precursor layer thickness on PEO coatings: Energy consumption and long-term corrosion performance. *Surface and Coatings Technology*. 2024, 476: 130186.
 34. Chandrabhan Verma, Shikha Dubey, Ranjith Bose, Akram Alfantazi, Eno E. Ebenso, Kyong Yop Rhee: Zwitterions and betaines as highly soluble materials for sustainable corrosion protection: Interfacial chemistry and bonding with metal surfaces. *Advances in Colloid and Interface Science*. 2024, 324: 103091.
 35. Guihua Li, Lei Chen, Yulong An, Meizhen Gao, Huidi Zhou, Jianmin Chen: Investigating the effect of polytetrafluoroethylene on the tribological properties and corrosion resistance of epoxy/hydroxylated hexagonal boron nitride composite coatings. *Corrosion Science*. 2023, 210: 110820.
 36. Daixiong Zhang, Lin Zhuo, Qing Xiang: Electrophoretic deposition of polytetrafluoroethylene (PTFE) as anti-corrosion coatings. *Materials Letters*. 2023, 346: 134524.
 37. Qiao Zhang, Aijie Ma, Binghong Zhang, Shibo Liang, Yuming Chen, Qiaoyin Li, Xinmeng Mao, Weifeng Zhao, Hongwei Zhou: NIR photoresponsive shape memory polyurethanes composite with selfhealing and anti-corrosion properties. *Polymer*. 2024, 299: 126957.
 38. Shicheng Li, Yinjie Xu, Fuquan Xiang, Peng Liu, Haibo Wang, Wangru Wei, Shihua Dong: Enhanced corrosion resistance of selfhealing waterborne polyurethane coating based on tannic acid modified ceriummontmorillonites composite fillers. *Progress in Organic Coatings*. 2023, 178: 107454.
 39. Zexin Ye, Lei Guan, Yu Li, Jiabin Zhong, Lingchao Liao, Dingwei Xia, Jiayong Huang: Understanding the galvanic corrosion of Cu-Ni alloy/2205 DSS couple using electrochemical noise and microelectrochemical studies. *Corrosion Science*. 2023, 224: 111512.
 40. Yan Li, Tao Zhang, Fuhui Wang: Unveiling the effect of Al-Mn intermetallic on the micro-galvanic corrosion of AM50 Mg alloy in NaCl solution. *Journal of Materials Research and Technology*. 2023, 26: 753-763.